THE AMERICAN SOCIETY OF MECHANICAL ENGINEERS
345 E. 47th St., New York, N.Y. 10017

97-GT-316

Characterizing the Effects of Air Injection on Compressor Performance for Use in Active Control of Rotating Stall

Robert L. Behnken*†‡ Mina Leung‡ Richard M. Murray‡
Division of Engineering and Applied Science
California Institute of Technology
Pasadena, CA

Abstract

Previous work has developed an air injection controller for rotating stall based on the idea of a shifting compressor characteristic and the Moore-Greitzer three state compressor model. In order to demonstrate this form of control experimentally, a series of open loop tests were performed to measure the performance characteristics of a low speed axial flow compression system when air is injected upstream of the rotor face. The position of the air injection port relative to the hub and the rotor face and the angle relative to the mean axial flow were varied. The tests show that the injection of air has drastic effects on the stalling mass flow rate and on the size of the hysteresis loop associated with rotating stall. The stalling mass flow rate was decreased by 10% and the hysteresis loop was completely eliminated under some conditions. The results of the open loop parametric study were then used to implement a closed loop control strategy based on a shifting characteristic.

1 Introduction

As gas turbine engines have become better understood and better designed, active control has become a more attractive method for increasing performance. Initial efforts at including control involved open loop scheduling systems such as that presented by Gilyard and Orme [5]. These control systems varied engine parameters quasi-statically as the engine transitions between operating regions and experimentally demonstrated substantial performance increases. The desire for still higher performance and greater efficiency, as well as improved sensing, actuation, and greater computation capability, have driven research into active control techniques.

Two of the limiting factors in the performance of compression systems are rotating stall and surge. Rotating stall refers to a dynamic instability that occurs when a nonaxisymmetric flow pattern develops in the blade passages of a compressor stage and results in a drastic reduction in the performance of the system. This degradation in performance is usually unacceptable and must be avoided. Surge is a large amplitude, axisymmetric oscillation in the compressor which results from exciting unstable dynamics in the overall pumping system. While surge and stall are separate phenomenon, the presence of stall is often precursor to the onset of surge in many compression systems. The compressor model developed by Moore and Greitzer [13] has provided controls researchers with a tractable model for controller design which qualitatively captures rotating stall and surge.

Several active control techniques have been demonstrated experimentally that decrease the detrimental effects of rotating stall in axial flow compressors; these include inlet guide vanes [14] and air injection [3, 7]. Each of these schemes involved active cancellation of measured flow or static pressure perturbations upstream of the rotor. More recently, active control using air injection was demonstrated on a full scale engine using linear control techniques by Weigl et al. [15]. A study of different actuation techniques performed in [8] based on a linear analysis of the Moore and Greitzer model provided additional theoretical basis for the cancellation approaches.

Based on the Moore and Greitzer model, there are two additional methods for controlling rotating stall and surge which do *not* depend directly on active cancellation of upstream perturbations. The first of these is based on modulation of the throttle characteristic and was first explored theoretically by Liaw and Abed [10] and demonstrated experimentally by Eveker et al. [4]. The second method (which will be exploited here) involves modulation of the compressor characteristic. It is important to note that these two control strategies are axisymmetric and are based on the changing the bifurcation behavior of the open loop system through feedback.

Previous theoretical work based on the Moore-Greitzer three state compressor model suggested that if an actuator can be found which changes the compressor performance characteristic, this effect could be used to control the growth of rotating stall cells (see [2]). Air injection actuators placed upstream of the rotor face have this capability.

In order to apply this control technique, open loop experiments were performed to characterize how con-

*This material is based upon work partially supported under a NSF Graduate Research Fellowship.

†1Lt USAF, WL/MNAG, 101 W Eglin Pkwy. Ste 334, Eglin AFB FL 32542-6810.

‡Funding for this research was provided in part by AFOSR grant F49620-95-1-0409.

Presented at the International Gas Turbine & Aeroengine Congress & Exhibition
Orlando, Florida — June 2-June 5, 1997

tinuous air injection changed the performance characteristic on a low speed rig at Caltech. The resulting parametric study identified how different geometric parameters associated with the air injection affected the rig performance. In the work presented here, the angle at which air was injected relative to the axial flow direction and the span-wise position at which the injected air reached the rotor face were both varied. In addition, experiments were performed with reduced amounts of injected air in order to determine the minimal amount of injection required to achieve rotating stall control.

This paper is organized as follows. Section 2 describes the theoretical basis for the shifting compressor characteristic control strategy. Section 3 describes the Caltech compressor rig and the air injection actuators. Section 4 presents the open-loop parametric study on how the compressor performance characteristic is affected as the injection parameters (injection angle and span-wise position). Section 5 combines the open loop experimental results with the theoretical results presented Section 2 to implement a rotating stall controller. Finally, Section 6 summarizes the results of the paper and suggests some areas of future work.

2 Theoretical Basis

The Moore–Greitzer three state model for rotating stall and surge in axial flow compressors was originally presented in [13], and the basic fluid mechanics assumptions in the model can be obtained there. Note that throughout this paper flow coefficients will be normalized by the mean rotor speed, V_m (the speed of the rotor at mid-span), and pressure rise coefficients will be normalized by $\frac{1}{2}\rho V_m^2$ where ρ is the density of air.

2.1 Moore–Greitzer Model

The following set of ODEs describe the dynamics of the compression system:

$$\begin{aligned}\frac{d\Psi}{d\xi} &= \frac{1}{4l_cB^2}\left(\Phi - \gamma\sqrt{\Psi}\right)\\ \frac{d\Phi}{d\xi} &= \frac{1}{l_c}\left(\Psi_c(\Phi) - \Psi + \frac{J_1}{4}\frac{\partial^2\Psi_c}{\partial\Phi^2}\right)\\ \frac{dJ_1}{d\xi} &= \frac{2}{\mu+2}J_1\left(\frac{\partial\Psi_c}{\partial\Phi} + \frac{J_1}{8}\frac{\partial^3\Psi_c}{\partial\Phi^3}\right),\end{aligned} \tag{1}$$

where Ψ is the average pressure rise coefficient, Φ is the average flow coefficient, J_1 is the square amplitude of the sinusoidal flow coefficient perturbation, ξ is dimensionless time, Ψ_c is the steady state compressor characteristic, γ is the throttle coefficient (denoting the amount of throttle opening), and l_c, B, and μ are parameters which depend on the compression system. The steady state compressor characteristic $\Psi_c(\Phi)$ is parameterized as

$$\Psi_c(\Phi) = a_0 + a_1\Phi + a_2\Phi^2 + a_3\Phi^3. \tag{2}$$

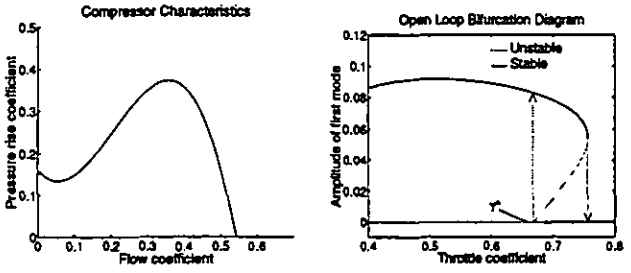

Figure 1: Bifurcation diagram showing jumps associated with the hysteresis loop for an open loop compression system with the characteristic shown at the left (pure rotating stall case).

For further details on the development of this model see the original work by Moore and Greitzer [6, 13].

The bifurcation behavior of system (1) has been explored by McCaughan [11, 12] and Abed et al. [1]. The analytical results showed that the model exhibits surge (which corresponds to a Hopf bifurcation) and rotating stall (which corresponds to a transcritical bifurcation). In addition, the experimentally observed hysteresis associated with rotating stall is also captured; this is shown by the bifurcation diagram for J_1 versus the throttle coefficient, γ, presented in Figure 1. In the figure the unstable equilibria are shown as grey lines, and the stable equilibria are shown as black lines. The diagram suggests a hysteresis region since as the throttle is closed (γ is decreased) $J_1 = 0$ is a stable solution until γ^* is reached, at which point the stable solution for J_1 is non-zero (which corresponds to a jump to rotating stall). The system has substantially different solutions depending on the path that γ follows. Further details on the bifurcation behavior of system (1) can be found in [11, 12].

Several rotating stall controllers have been proposed based on system (1) that work by changing the shape of the bifurcation diagram shown in Figure 1. Throttle controller by Liaw and Abed [10] and by Krstić et al. [9] and an air injection controller by Behnken et al. [2]. The work here focuses on using the air injection controller and more details on the behavior of this control law will be presented later.

2.2 Compressor Characteristic Shift

Based on the experimental results described in [2] we model direct actuators of the steady state compressor characteristic. Here we present previous results from [2] for the closed loop system where the feedback is proportional to the size of the first mode of the stall cell squared:

$$\Psi_c = \Psi_{c_{nom}} + KJ_1\Psi_{c_u} \tag{3}$$

where

$$\Psi_{c_{nom}} = a_0 + a_1\Phi + a_2\Phi^2 + a_3\Phi^3 \tag{4}$$

and

$$\Psi_{c_u} = c_0 + c_1 \Phi. \tag{5}$$

A shifting of the steady state compressor characteristic curve proportional to J_1 can change the character of the bifurcation shown in Figure 1. To see how, we first solve for the slope of the bifurcation curve at the point γ^*. On the stalled branch of the bifurcation diagram, the following algebraic equations must hold:

$$\Phi^2 = \gamma^2 \Psi, \tag{6}$$

$$\Psi_c = \Psi - \frac{J_1}{4} \frac{\partial^2 \Psi_c}{\partial \Phi^2}, \tag{7}$$

and

$$\frac{\partial \Psi_c}{\partial \Phi} = -\frac{J_1}{8} \frac{\partial^3 \Psi_c}{\partial \Phi^3}. \tag{8}$$

Noting that, for each equilibrium solution on the stalled branch of the bifurcation diagram, choosing J_1 fixes Φ, Ψ, and γ, and hy differentiating equation (6) with respect to J_1 we obtain

$$2\Phi \frac{d\Phi}{dJ_1} = 2\gamma\Psi \frac{d\gamma}{dJ_1} + \gamma^2 \frac{d\Psi}{dJ_1}. \tag{9}$$

By differentiating equation (7) with respect to J_1, an expression for $\frac{d\Psi}{dJ_1}$ at the peak of the compressor characteristic is found to be

$$\left.\frac{d\Psi}{dJ_1}\right|_{\gamma=\gamma^*} = K\Psi_{c_u} + \frac{1}{4} \frac{\partial^2 \Psi_{c_{nom}}}{\partial \Phi^2}. \tag{10}$$

By similar differentiation of equation (8) with respect to J_1, an expression for $(d\Phi/dJ_1)$ at the same point is found to be

$$\left.\frac{d\Phi}{dJ_1}\right|_{\gamma=\gamma^*} = \frac{K\frac{\partial \Psi_{c_u}}{\partial \Phi} + \frac{1}{8}\frac{\partial^3 \Psi_{c_{nom}}}{\partial \Phi^3}}{-\frac{\partial^2 \Psi_{c_{nom}}}{\partial \Phi^2}}. \tag{11}$$

If equations (10) and (11) are substituted into equation (9) and the result solved for $(dJ_1/d\gamma)$, the slope of the bifurcation diagram at the equilibrium point associated with γ^* is obtained as:

$$\left.\frac{dJ_1}{d\gamma}\right|_{\gamma=\gamma^*} = \frac{\sqrt{\Psi}}{\frac{K\Psi'_{c_u} + \frac{1}{8}\Psi'''_{c_{nom}}}{-\Psi''_{c_{nom}}} - \frac{\Phi\left(K\Psi_{c_u} + \frac{1}{4}\Psi''_{c_{nom}}\right)}{2\Psi}}, \tag{12}$$

where all expressions in the right hand side of equation (12) are evaluated at the equilibrium point at the peak of the compressor characteristic, and $(\,)'$ denotes partial differentiation of $(\,)$ with respect to Φ.

From this expression it is easy to see how varying the gain on the shifted characteristic affects the slope of the bifurcation diagram at γ^*. Typically, $(dJ_1/d\gamma)|_{\gamma=\gamma^*}$ is positive (as is shown in the bifurcation diagram in Figure 1) and if this positive value were increased, the size of the hysteresis region could be decreased. If the shifted portion of the characteristic, Ψ_{c_u}, has a positive offset term ($c_0 > 0$) the slope will be increased by a positive gain K, and if the shifted characteristic has a negative linear term ($c_1 < 0$) the slope will also be increased for a positive gain K. Figure 2 shows how the bifurcation diagram changes as the gain K for a model of the Caltech rig.

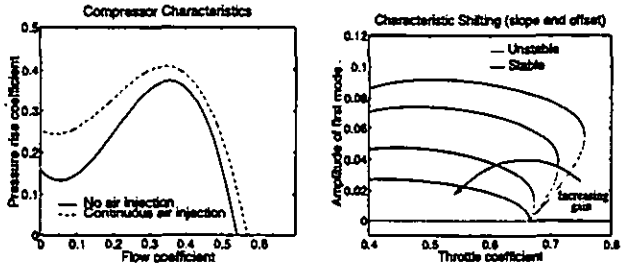

Figure 2: Bifurcation diagram for the shifting of compressor characteristic control law given in equation (3).

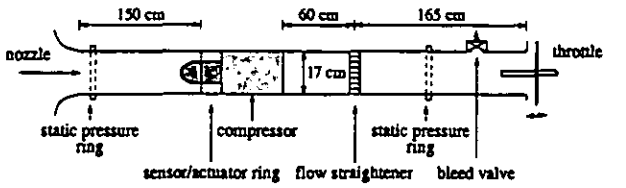

Figure 3: Caltech rig in rotating stall configuration.

The above analysis applies to any physical mechanism which can be used to change the compressor performance characteristic. Some other possible methods of achieving a shift in the compressor characteristic include active casing treatments and hub distortion. The optimal choice of shift would be as described, and equation (12) would show the tradeoff of varying the slope versus the offset. In this paper, shifts in the compressor characteristic obtained using air injection will be used to implement this control strategy.

3 Experimental Description

Previous work on using pulsed air injectors to control rotating stall was presented in [2]; initial work towards locating an optimal controller was presented there as well as a complete description of the Caltech compression system. A short summary of that work is presented here in order to present further experimental results.

A schematic of the Caltech compressor rig is shown in Figure 3. The compressor itself is an axial flow compressor driven hy an electric motor. The rig is instrumented with pressure transducers 5 cm (0.7 mean rotor radii) upstream of the rotor which are used to determine the amplitude of the first and second modes of the static pressure perturbation produced by the rotating stall. Additional pressure sensors are used to determine the annulus averaged pressure rise and flow rate, and a PC-based data acquisition system was used for the experiments presented here. The rig was operated at a

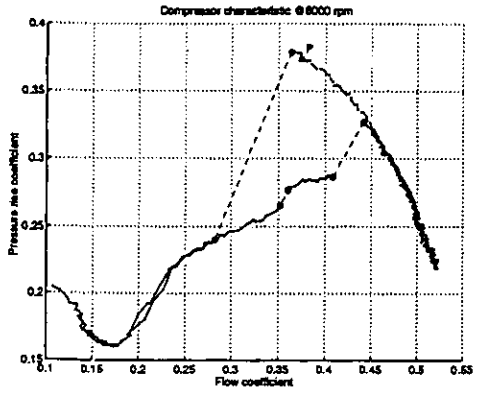

Figure 4: Caltech rig compressor characteristic. Dark lines indicate continuous changes in the operating point while lighter lines represent discontinuous changes.

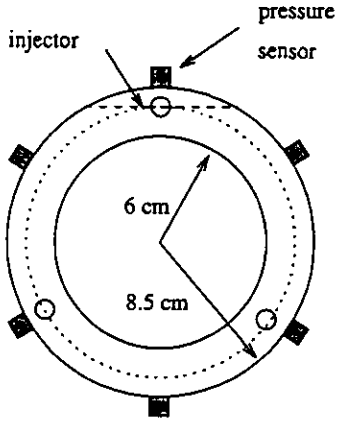

sensor ring (end view)

Figure 5: Parametric study details. The dashed line shows how the injection position was varied for the plots presented by D'Andrea et al [2] which were reproduced in Figure 7 and the dotted line shows how the injection position was varied for the plots in Figures 8 and 9.

rotor speed of 6000 RPM which corresponds to a mass flow of 0.19 m^3/sec and a pressure rise of 940 Pa at the peak of the steady state compressor characteristic (see Figure 4). The frequency of the first mode of fully developed rotating stall for this rig under these operating conditions is 64.5 Hz. Three air injectors placed 120 degrees apart around the compressor annulus 9 cm (1.25 mean rotor radii) upstream of the rotor were used as actuators, and each of these injectors had a maximal control authority of 1.7% relative to the total mass flow through the compressor. For further information about the system see [2].

Figure 5 shows a schematic of how the air injectors are physically placed in the compressor annulus and shows each of the three geometric parameters described above. In the studies presented here, only the angle relative to the mean axial flow and the span wise position of the air injection were varied. All combinations of air injection angles and span positions were not possible with the current experimental apparatus because if interference with the inlet nose cone. In addition, the air injectors did create a blockage upstream of the rotor

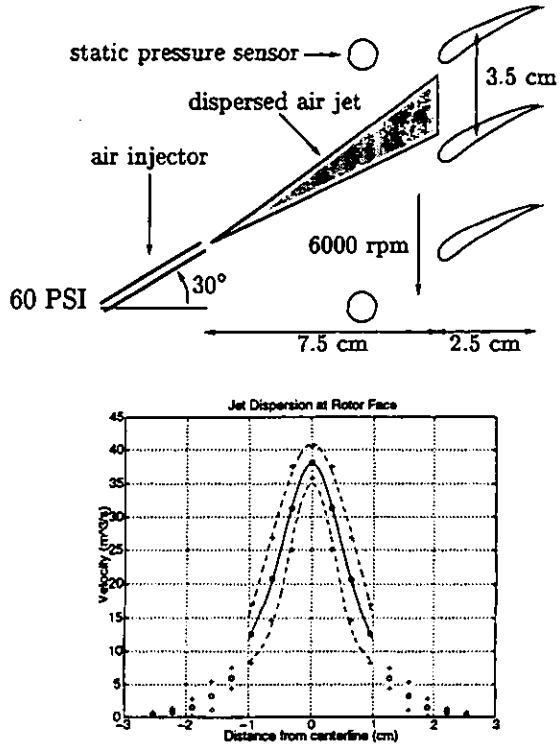

Figure 6: Air injection geometry and velocity profile of the injected air at the compressor face.

Figure 6 shows the velocity profile (with uncertainty shown by a dashed line) of the injected air when it reaches the rotor face (1.25 mean rotor radii from the air injection port exit).

4 Open Loop Experiments

The focus of these experiments was to determine how air injection upstream of the rotor can affect the stall characteristics of the compressor. Figure 7 shows examples of how the steady compressor performance characteristic can be changed by continuous air injection; these figures where originally presented by D'Andrea et al. [2] and were obtained by injecting approximately 5% of the mean mass flow through the compressor at different span-wise positions and at different angles relative to the mean axial flow. The key aspect of this figure is the wide range of performance characteristics which were obtained using the same amount of air injection. The experiments presented here separate the effects of span-wise injection position versus injection angle. The shift of the compressor characteristic obtained by con-

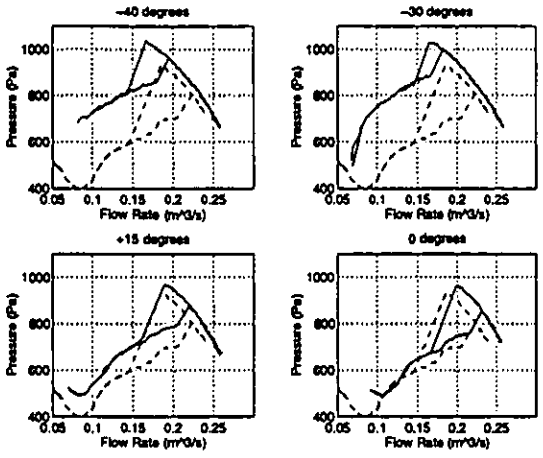

Figure 7: The compressor characteristic obtained for different air injection positions is shown as a solid line. For comparison, the compressor characteristic obtained with no air injection is shown as a dashed line. (Plot reproduced from [2].)

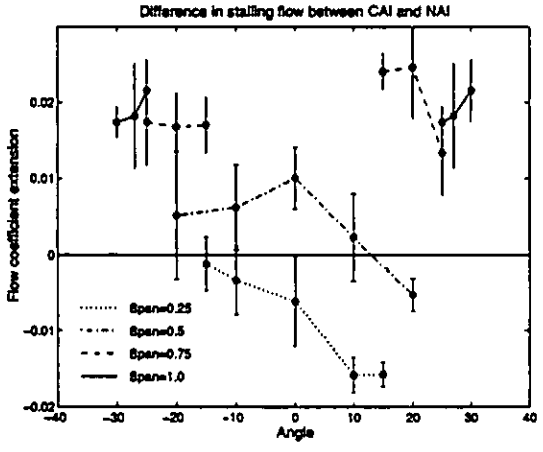

Figure 8: Air injection parametric study of geometric parameters: change in stalling flow coefficient.

tinuous air injection can be described by two parameters, the amount that the stall point is moved and the change in the size of the hysteresis loop.

After the geometric parameters of the air injection have been established to shift the compressor characteristic in a useful way (see Section 2), these shifts will be used for closed loop control. The purpose of the open loop experiments is to identify shifts of the compressor performance characteristic which are available on the Caltech rig so that the control law can be demonstrated experimentally.

4.1 Stall point location

Figure 8 shows how the stalling flow rate is extended for various injection angles and span-wise injection heights.

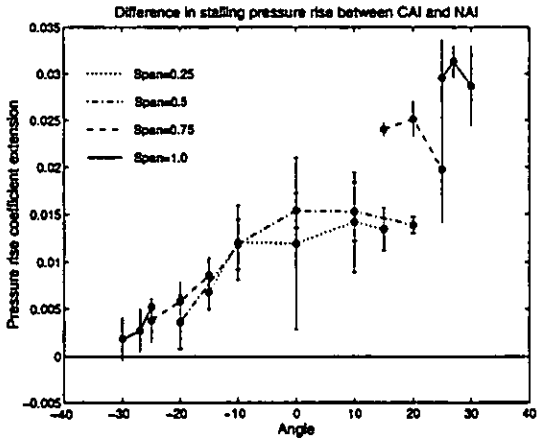

Figure 9: Air injection parametric study of geometric parameters: change in pressure rise at stall point.

The plot shows the difference between stalling flow coefficient for the uninjected case and the continuous air injection case. Lower stalling flow rates than the uninjected case are shown as positive values. The results indicate that the greatest extensions occur at large injection angles and at near 100% span (i.e. at the tip).

In addition to the stalling flow coefficient, the presure rise coefficient at the stall point is also affected by the air injection. Figure 9 shows the change in the pressure rise coefficient delivered by the system as a function of the injection angle and span-wise position. Again the results are plotted as the difference between the stalling pressure rise for the uninjected case and the injected case. Positive values in the plot correspond to the injected case providing higher pressure rise than the uninjected case. The plot shows that the greatest extension occurs for positive injection angles and 100% span injection.

4.2 Size of hysteresis region

Figure 10 shows the size of the hysteresis region for different air injection parameters. The plot shows the difference between the amount that the throttle coefficient must be varied to clear the rotating stall for the no air injection case and the amount that the throttle coefficient must be varied to clear the rotating stall for the air injected case. In this case the throttle coefficient γ_e is defined as:

$$\gamma_e = \frac{\Phi_e}{\sqrt{\Psi_e}} \tag{13}$$

where the Φ_e is the equilibrium mean axial flow coefficient and Ψ_e is the equilibrium plenum pressure rise coefficient.

The optimal choice for geometric location of the air injectors for closed loop experiments, based on the analysis presented by Behnken et al. [2], would be positive injection angle around 30 degrees at the tip of the rotor.

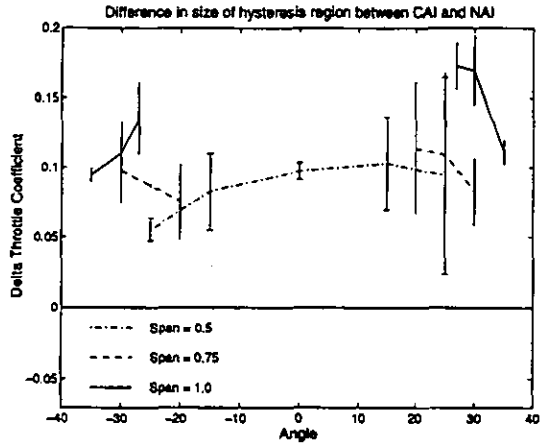

Figure 10: Air injection parametric study of geometric parameters: change in size of hysteresis region.

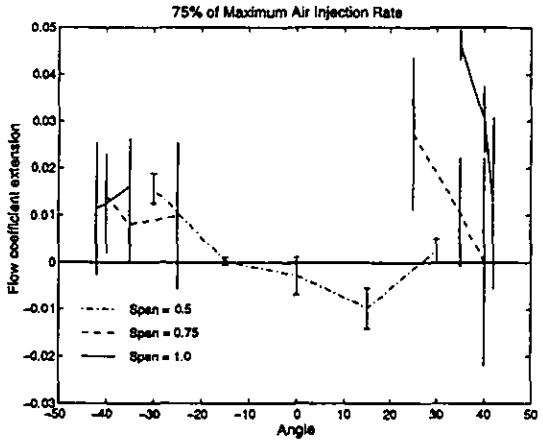

Figure 11: Flow extension for low flow condition with close coupled air injection.

This corresponds to the greatest reduction in the size of the rotating stall hysteresis loop.

4.3 Reduced injection flow rate

In the second parametric study, the amount of injected air is varied in order to determine the minimum amount of injection required to achieve the decrease in stalling flow rate and the reduction in the size of the hysteresis loop. This study is of particular interest because the viability of air injection actuation on real gas turbine engines depends on using very low amounts of injection.

For this parametric study, the air injection flow rate was set to 75% of the maximum, and the angle and span position of the injected air was varied as in the previous study. Figures 11 and 12 show that for lower air injection flow rates the trend observed under the previous conditions still holds; the optimal choice for geometric location of the air injectors for closed loop experiments, would be positive injection angle around

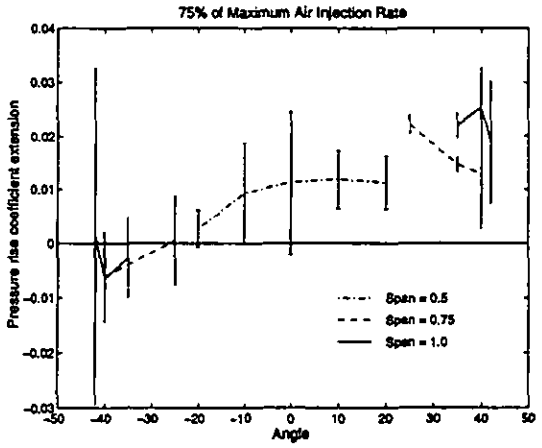

Figure 12: Pressure rise extension for low flow condition with close coupled air injection.

30 degrees at the tip of the rotor.

As the figures in this section suggest, all combinations of air injection angles and span positions were not possible with the current experimental apparatus. This was because if interference with the inlet nose cone. In addition, the air injectors did create a blockage upstream of the rotor which varied based on the position and orientation of the air injectors. This blockage varied from 1-3% of the total area of the compressor annulus, but does not explain the changes in the stall point or size of the hysteresis. For example, Figures ?? and 12 asymmetry between positive and negative air injection angles, but the amount of blockage depends only on the magnitude of the injection angle, not on the sign.

5 Closed Loop Experiments

In order to test the closed loop compressor characteristic shifting idea presented in Section 2, a series of experiments were performed. The control scheme presented there was based on a shift of the nominal compressor characteristic which was proportional to the amplitude of the first mode amplitude of the rotating stall, (see equation (3)). In order to achieve this proportional feedback on the amplitude of the stall cell magnitude, the duty cycle of the air injectors was varied. A carrier frequency of 100 Hz was used (selected to be as higb as possible while still obtaining stable performance for the air injector valves), with the duty cycle varying between 0–100% proportional to the amplitude of the static pressure perturbation amplitude (obtained using the static pressure transducers located 0.7 rotor radii upstream of the rotor face). Two compressor characteristic shifts were investigated for closed loop experiments, one with a rotating stall hysteresis region that did not overlap that of the uninjected case and one with a hysteresis region that did overlap.

Figure 13 shows the closed loop compressor characteristic obtained for the non-overlapping hysteresis re-

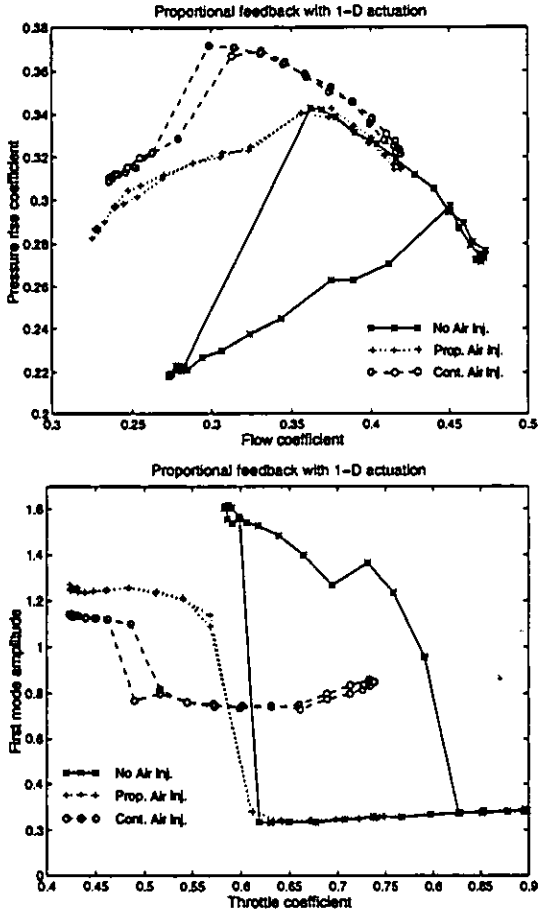

Figure 13: Closed loop compressor characteristic and bifurcation diagram, obtained with 1–D proportional feedback: non-overlapping hysteresis case.

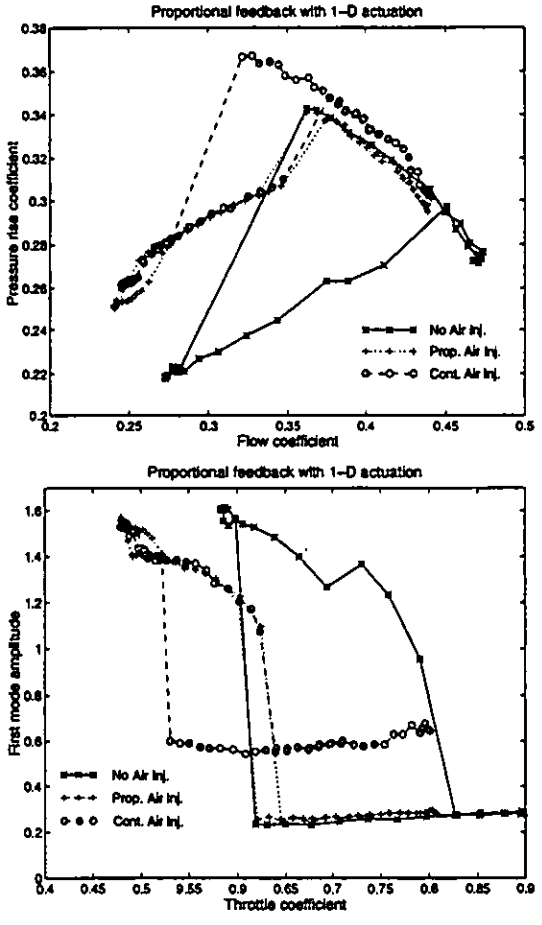

Figure 14: Closed loop compressor characteristic and bifurcation diagram obtained with 1–D proportional feedback: overlapping hysteresis case.

gion case (top plot), along with an experimental bifurcation diagram (bottom plot). The bifurcation diagram shows that the entire nonzero rotating stall equilibria branch is stable, and there is therefore no hysteresis region associated with the rotating stall. This case is in agreement with the analytical analytic results presented in Section 2.

Figure 14 shows the closed loop compressor characteristic ohtained for the overlapping hysteresis region case (top plot), along with an experimental bifurcation diagram (bottom plot). The experimental bifurcation diagram shows the effects of saturation described in [2]. The hysteresis region is as would be expected from the analysis presented there.

While the size of the hysteresis region for the closed loop system is as the analysis predicts, no new small amplitude rotating stall solutions were observed (the theory predicts that there should be some prior to transition to rotating stall). One possible explanation for this discrepancy is that the gain for the proportional control was not large enough. The experimental search for these new small amplitude rotating stall equilibria was not exhaustive, and there is room for more investigation of this phenomenon.

The experimental bifurcation diagrams for the continuous air injection case show that the air injection introduces a large amount of non-axisymmetric flow disturbance. This is evident in both the non-overlapping and overlapping hysteresis cases, and is one reason that the active control strategy is better than simply using continuous air injection. In other words, with the active injection scheme the flow perturbations are introduced only when necessary.

Based on the Moore–Greitzer three state model, a controller based on an axisymmetric compressor characteristic shift behaves very similarly to what was observed in these experiments. This suggests that other control methods which would rely on a compressor performance characteristic shift as a means of active control could be modeled in the same way. The analysis in Section 2 is general enough that it captures any mechanism for producing the shift from the nominal compres-

sor characteristic $\Psi_{c_u}(\Phi)$. Some other possible methods of achieving a shift in the compressor characteristic include active casing treatments and hub distortion.

6 Conclusions and Future Work

Based on previous theoretical work which suggested that if an actuator can be found which changes the compressor performance characteristic in a particular way, this effect can be used to control the growth of rotating stall cells (see Section 2 or [2]), open loop experiments were performed to characterize how continuous air injection changed the performance characteristics for the Caltech rig. The resulting parametric study identified how different geometric parameters associated with the air injection affected the rig performance. In the work presented here, the angle at which air was injected relative to the axial flow direction was varied and the spanwise position at which the injected air reached the rotor face were both varied. In addition, experiments were performed with reduced amounts of injected air in order to determine the minimal amount of injection required to achieve rotating stall control.

It was found that the stalling mass flow could be reduced by injecting air near the tip of the rotor face at an angle of nearly 30 degrees relative to the mean flow direction. In addition, the hysteresis region associated with rotating stall was completely eliminated for the same parameter choices.

It was also found that similar trends to those found for the maximum air injection flow rates were also present for a flow rate of 75% of the maximum if the air injection port was moved closer to the rotor face. This result is promising because it shows that there is room to further reduce the amount of mass and momentum required for active control of rotating stall.

Closed loop experiments were performed which support the simple compressor characteristic shifting model for the control of rotating stall presented in [2]. The two cases investigated (non-overlapping hysteresis and overlapping hysteresis) both agree with the theoretical results for the size and shape of the rotating stall hysteresis region.

The MG–3 model of control using an axisymmetric compressor characteristic shift behaves very similarly to what was observed in these experiments. This suggests that other control methods which would rely on a compressor performance characteristic shift as a means of active control could be modeled in the same way. The analysis in Section 2 is general enough that it captures any mechanism for producing the shift from tbe nominal compressor characteristic $\Psi_{c_u}(\Phi)$. Some other possible methods of achieving a shift in the compressor characteristic include active casing treatments and hub distortion. Areas of future work include attempting this sort of axisymmetric control strategy on multi-stage or high speed rigs and identifying and demonstrating other methods of obtaining the characteristic shifts such as those described.

References

[1] E. H. Abed, P. K. Houpt, and W. M. Hosny. Bifurcation analysis of surge and rotating stall in axial flow compressors. *Journal of Turbomachinery*, 115:817–824, October 1993.

[2] R. D'Andrea, R. L. Behnken, and R. M. Murray. Active control of an axial flow compressor via pulsed air injection. CDS Technical Report 95-029, Caltech, 1995. (To appear *Journal of Turbomachinery*).

[3] I. J. Day. Active supression of rotating stall and surge in axial compressors. *Journal of Turbomachinery*, 115:40–47, 1993.

[4] K. M. Eveker, D. L. Gysling, C. N. Nett, and O. P. Sharma. Integrated control of rotating stall and surge in aeroengines. In *Sensing, Actuation, and Control in Aeropropulsion; SPIE 1995 International Symposium on Aerospace/Defense Sensing and Dual-Use Photonics*, pages 21–35, 1995.

[5] G. B. Gilyard and J. S. Orme. Subsonic flight test evaluation of a performance seeking control algorithm on an F-15 airplane. In *Joint Propulsion Conference and Exhibit*, pages AIAA paper 92–3743, 1992.

[6] E. M. Greitzer and F. K. Moore. A theory of post-stall transients in axial compression systems—Part II: Application. *Journal of Turbomachinery*, 108:231–239, 1986.

[7] D. L. Gysling. *Dynamic Control of Rotating Stall in Axial Flow Compressors Using Aeromechanical Feedback*. PhD thesis, Department of Aeronautics and Astronautics, Massachusetts Institute of Technology, Cambridge, Massachusetts, 1993.

[8] G. J. Hendricks and D. L. Gysling. Theoretical study of sensor-actuator schemes for rotating stall control. *Journal of Propulsion and Power*, 10(1):101–109, 1994.

[9] M. Krstić, I. Kanellakopoulos, and P. Kokotović. *Nonlinear and Adaptive Control Design*. John Wiley and Sons, 1995.

[10] D. C. Liaw and E. H. Abed. Control of compressor stall inception: A bifurcation-theoretic approach. *Automatica*, 32(1):109–115, 1996.

[11] F. E. McCaughan. Application of bifurcation theory to axial flow compressor instability. *Journal of Turbomachinery*, 111:426–433, 1989.

[12] F. E. McCaughan. Bifurcation analysis of axial flow compressor stability. *SIAM Journal of Applied Mathematics*, 20(5):1232–1253, 1990.

[13] F. K. Moore and E. M. Greitzer. A theory of post-stall transients in axial compression systems—Part I: Development of equations. *Journal of Turbomachinery*, 108:68–76, 1986.

[14] J. D. Paduano, A. H. Epstein, L. Valavani, J. P. Longley, E. M. Greitzer, and G. R. Guenette. Active control of rotating stall in a low-speed axial compressor. *Journal of Turbomachinery*, 115:48–56, January 1993.

[15] H. Weigl, J. Paduano, A. Epstein, E. Greitzer, M. Bright, and A. Strazisar. Active stabilization of rotating stall in a transonic single stage axial compressor. In *To Appear Proc. ASME Turbo Expo*, 1997.